agriculture

MDPI

Article

Optimal Relationship Between As and Cd in Porewater of Paddy Soils with Variations in pe + pH: Insight from Trade-Off Value Analysis

Xiaosong Tian [1,*,†], Jiahang Li [2,†], Guanqun Chai [3,*], Dayong Luo [1], Yalong Gong [4], Huang Liu [4], Qing Xie [1] and Guanghui Li [4]

[1] College of Resources and Safety, Chongqing Vocational Institute of Engineering, Chongqing 402260, China; dayluo@163.com (D.L.); cqxqing@163.com (Q.X.)
[2] College of Resources and Environment, Southwest University, Chongqing 400715, China; 18202850327@163.com
[3] Institute of Soil and Fertilizer, Guizhou Academy of Agricultural Sciences, Guiyang 550006, China
[4] Chongqing Engineering Research Center for Soil Contamination Control and Remediation, Chongqing 400067, China; gongyalong@cmhk.com (Y.G.); liuhuang@cmhk.com (H.L.); liguanghui@cmhk.com (G.L.)
* Correspondence: tianxs@cqvie.edu.cn (X.T.); chaiguanqun@163.com (G.C.)
† These authors contributed equally to this work.

Abstract: The remediation of paddy soils co-contaminated with As and Cd is tricky. It is difficult to decrease Cd and As availability simultaneously due to their opposite geochemical characteristics. Finding the optimal trade-off relationship between As and Cd availability in paddy soils is a significant task that is necessary to guide the construction of water management measures. This study investigated the dissolution characteristics of As, Cd, Fe, Mn, DOC, DOM, and various As and Cd fractions in soils via the microcosm system and calculated the optimal trade-off value for available As and Cd in porewater. The results showed that the total As in porewater increased rapidly when the soil Eh was reduced to −104 mV. Meanwhile, the total Cd in porewater decreased dramatically when the soil Eh was below 62 mV. Under flooding and drainage conditions, Fe/Mn (oxyhydro)oxides play a vital role in regulating Cd dissolution in paddy soils, while Fe/Mn (oxyhydro)oxides organically bind sulfide together to determine the dissolution of As. Additionally, the optimal pe + pH response to the minimum trade-off value of available As and Cd in porewater was found to be 6.6, which indicates a moderate reduction status. Therefore, further research should apply the optimal pe + pH to construct water management measures to safely utilize co-contaminated paddy fields.

Keywords: water management; dissolved As and Cd; dissolved organic matter; Fe/Mn (oxyhydro)oxides; pe + pH; trade-off value

Citation: Tian, X.; Li, J.; Chai, G.; Luo, D.; Gong, Y.; Liu, H.; Xie, Q.; Li, G. Optimal Relationship Between As and Cd in Porewater of Paddy Soils with Variations in pe + pH: Insight from Trade-Off Value Analysis. *Agriculture* **2024**, *14*, 1933. https://doi.org/10.3390/agriculture14111933

Academic Editor: Dongdong Yan

Received: 21 September 2024
Revised: 27 October 2024
Accepted: 28 October 2024
Published: 30 October 2024

1. Introduction

The occurrence of cadmium (Cd) and arsenic (As) in soils is a significant risk to global food safety and human health due to their teratogenic and carcinogenic attributes. As a result, a substantial portion of the world's population is currently exposed to potential risks from agricultural products polluted with As and Cd [1–3]. Rice (*Oryza sativa* L.) is a staple food for about half of the world's population and is also a primary dietary source of As and Cd due to the high bioaccumulation of these elements [1,4]. Therefore, paddy soil and rice contaminated with As and Cd have received widespread attention [5,6], and both toxic elements have been recognized as priority pollutants in China [7]. However, while the accumulation of As and Cd is of roughly the same order of magnitude in rice, the ratio of grain to the soil's total element concentration of Cd is one to two orders of magnitude higher than that of As, indicating that Cd has a much higher transferability from soil to rice grain than As [8]. The difference in accumulations of As and Cd in rice is usually related to

their mobility and availability in paddy soils and the corresponding transport channels for As and Cd in paddy rice. [4].

Water management usually mediates soil redox conditions and further impacts the oxidation–reduction process of Fe/Mn (oxyhydro)oxides [9,10], sulfate–sulfide [11,12], and As(V)–As(III) [13], as well as the dissolution of dissolved organic matter (DOM) [13,14] in paddy soils, resulting in differences in their availability [3]. There is a widespread belief that the bioavailability of As and Cd in paddy soils will follow opposite trends due to the elements' distinct geochemical characteristics, depending on the transformation of the critical factors of Fe- and S-associated redox [15,16]. Many previous studies have shown ambiguous results regarding the contributions of the two elements' (Fe and S) transformations to the availability of As and Cd in paddy soil. Some research supports the idea that sulfate reduction substantially impacts Cd and As fractions in paddy soils. The transformation of SO_4^{2-} to S^{2-} in anaerobic conditions was shown to generate low-solubility compounds, such as CdS, FeAsS, and As_2S_3 [17–20]. Nevertheless, some scholars also believe that Fe/Mn (oxyhydro)oxides contribute much more to the regulation of As and Cd availability in paddy soils than sulfur for the following reasons: (1) the proportions of As and Cd combined with Fe/Mn (oxyhydro)oxides are higher than those with sulfide, and (2) the availability of soil As and Cd is significantly affected by the phase transition of (oxyhydro)oxides, namely phase transition between amorphous and crystalline iron (oxyhydro) oxides [9,21,22]. Therefore, under the processes of flooding and drainage, the contributions of iron and sulfur to the variations in As and Cd availability are currently unknown.

Typically, during the flooding process, the concentration of As in porewater shows an increasing trend, while Cd in porewater shows a decreasing trend. In the drainage condition, the opposite trend is observed [22]. To our knowledge, based on the changing trends, the fitted curves of the normalized concentration of As/Cd in porewater will inevitably have an intersection point so that the summation of the normalized concentrations of As and Cd in porewater is kept to a minimum value. This is called the trade-off value [3,16]. Therefore, the optimal soil Eh and pH associated with the minimum trade-off value may also exist, and they can facilitate the decrease in the dissolution of As and Cd in paddy soils [3,18] and further inhibit rice uptake in paddy soils co-contaminated with As and Cd [15,16]. The soil pH corresponding to the optimal trade-off value for available As and Cd is weakly acidic or neutral, and the Eh range is about −100 mV, with slight deviations from one study to another [3,16,18]. Generally, the variations in protons (H^+) and electrons (e) can be observed simultaneously during flooding and drainage. Therefore, it is best not to analyze Eh and pH in isolation, and the pe + pH as a comprehensive parameter is often used to evaluate the soil redox state [14,23]. Additionally, the pe + pH and trade-off coupling can directly reflect the quantitative relationship between the soil redox state and the trade-off value [22,24]. Previous research using pot experiments discussed the trade-off relationship between As and Cd versus pH or Eh in the porewater of paddy soils, but the quantitative relationship between the trade-off value and pe + pH has not been evaluated through microcosmic experiments. The primary objectives of this study were as follows: (1) to illustrate the variation in soluble As and Cd in porewater with various pe + pH induced by flooding and drainage treatments, exploring the quantitative relationship between the pe + pH and concentrations of As and Cd in porewater; (2) to determine the influence of variable pe + pH conditions on As and Cd fractions, discussing the critical factors in the soil matrix and its contribution to controlling the dissolutions of As and Cd in porewater; and (3) to develop a simplified model of Cd and As dissolutions during the flooding and drainage processes via the pe + pH versus the trade-off value, providing an optimal pe + pH to mitigate the dissolution behavior of Cd and As in paddy soils. This study will provide further insight into the optimal relationship between As and Cd in porewater undergoing water management measures.

2. Materials and Methods

2.1. Incubation Experiment

2.1.1. Soil Preparation

The test paddy soils co-contaminated by As and Cd were collected from a demonstration field (26°59′ N, 106°53′ E), Guizhou Province, China. The soil type was yellow loam paddy soil. The top 0–20 cm layer of paddy soil was gathered and transported to the greenhouse for natural air drying. After that, the air-dried soils were ground and sieved with a 10-mesh nylon screen for the later incubation experiment. The soil pH value and the soil organic matter (SOC), Fe, Mn, As, and Cd contents of the paddy soils were 6.56, 5.56%, 3.45%, 582.67 mg/kg, 31.73 mg/kg, and 0.85 mg/kg, respectively. The original contents of As and Cd in paddy soils exceeded the risk screening values recommended by the GB15618–2018, China [25]. To obtain more obvious results for discussion in this study, we performed an exogenous addition experiment, aging the paddy soils for six months. The exogenous addition experiment followed our previous approaches [26], and the ultimate contents of As and Cd in the paddy soils were around 56.99 ± 0.48 mg/kg and 4.03 ± 0.34 mg/kg, respectively.

2.1.2. Microcosm System Design

We conducted soil microcosm incubation experiments to evaluate the As and Cd activities in paddy soils during the watering–drying period. The incubation procedures simulated the occurrence of flooding and draining in a paddy field following the original microcosm method as described by Wang et al., with some modifications [10,27]. In brief, 500 g of air-dried paddy soil was placed into 1000 mL polyethylene plastic bottles, and deionized water was added to the bottles to achieve the flooding depths indicated by the experimental design to explore the dissolution characteristics of As and Cd in paddy soils under the various redox potentials. The microcosm system was equipped with a porewater collector with a 0.60 μm pore sampling head (Rhizon MOM, Rhizosphere Research Products, Wageningen, The Netherlands), which was installed horizontally 3 cm from the soil bottom, as shown in Figures S1 and S2. The microcosm system can measure the soil Eh and pH in situ. Two holes were made in the caps of each of the polyethylene plastic bottles using a 5 mm drill bit to ensure that the overlying water was connected with the atmosphere and the evaporation was negligible. Before twisting the cap, we covered the bottleneck with a layer of nylon cloth to prevent other pollutants from entering the bottle.

Experiment 1 adopted the aged paddy soils to investigate the dynamic changes in the soil pH, redox potential (Eh), and total or soluble elements (such as Cd, As, Fe, Mn, and DOC) in the porewater during a waterlogged incubation at 1 cm of overlying water. The incubation experiment lasted 28 days and the porewater samples were collected via the fixed sampling head every two days (denoted as 2d, 4d, 6d, 8d, 10d, 12d, 14d, 16d, 18d, 20d, 22d, 24d, 26d, and 28d), as shown in Figure S1. Experiment 2 was designed to investigate the dynamic changes in the soil pH, Eh, and soluble elements (such as Cd, As, Fe, and Mn) associated with the various depths of overlying water. The experiment included three conditions: a waterlogged incubation from 8 cm to 1 cm (named 8 cm, 6 cm, 4 cm, 2 cm, and 1 cm), wet incubation at 0 cm, and drained incubation with three conditions (named dry1, dry2, and dry3). It took eight weeks for the microcosm system to remain stable at a depth of 8 cm; thereafter, each incubation period (i.e., 8 cm, 6 cm, 4 cm, 2 cm, 1 cm, 0 cm, dry1, dry2, and dry3) was maintained for one week, as shown in Figure S2. Experiments 1 and 2 were carried out at a constant temperature of 25 °C. The sampling volume of porewater was 20 mL during the waterlogged incubation periods involving 1–8 cm of submerged water, and the sample volume was 10 mL during the wet (0 cm) and drainage (dry1–3) incubation periods. Three replicates were performed for each experimental treatment (each sampling period).

2.2. Sampling and Testing

2.2.1. Porewater Samples

This study used continuous sampling instead of destructive sampling to collect porewater samples from the microcosm system. The porewater samples were collected using a soil solution sampler (Rhizon) equipped with a 10 cm sampling tube with a 0.60 μm pore size. For each incubation, the soil Eh was immediately determined at ca. 4 cm under the soil surface using the pH/ORP meter (PHSJ-6L, Shanghai Leici, Shanghai, China) assembled with a TR-901 ORP electrode (Shanghai Leici, Shanghai, China). The soil pH was measured with a pH/ORP meter assembled with an E-201-L pH combined electrode (Shanghai Leici, Shanghai, China) in unfiltered porewater. The collected porewater was divided into two portions (i.e., unfiltered and filtered porewater). The unfiltered solution was used to determine the concentrations of total As, Cd, Fe, and Mn in the porewater, and the solution filtered with a 0.45 μm filter membrane was used to measure the concentrations of soluble As, Cd, Fe, Mn, and DOC in porewater. The total Cd concentration in the unfiltered porewater was determined using inductively coupled plasma mass spectrometry (ICP-MS, Agilent 7900, Santa Clara, CA, USA) after the electrothermal plate digestion with the hybrid solution of H_2O_2 and HNO_3 (volume ratio, *v*:*v* = 1:2.5) at 250 °C. The soluble Cd in the filtered porewater samples was measured using the ICP-MS after the acidification of samples with concentrated HNO_3 to keep 2% acidity (*v*/*v*). An X-ray fluorescence spectrometer (XRF, JP500, JPscientific, Jiangsu, China) was used to determine the total and soluble As, Fe, and Mn in the porewater. The detection limit of ICP-MS for Cd in the aqueous solution was 0.05 μg/L, and the detection limit of XRF-JP500 for As in the aqueous solution was 0.01 mg/L. During the measurement process, we used the As and Cd standard solution (purchased on the Tansoole platform, https://www.tansoole.com/, accessed on 10 December 2023) as the reference material to calculate the recovery rates of As and Cd, evaluating quality assurance and quality control (QA/QC). The recovery rate of the elements ranged between 90 and 110%.

2.2.2. Soil Samples

After incubation, soil samples from various water management experiments (8 cm, 1 cm, and dry3) were collected and freeze-dried, and they were prepared with less than 100 mesh. The prepared soil samples (<100 mesh) were used to determine the total contents and fractions of As and Cd. The total contents of As and Cd in paddy soils were determined using two versions of the XRF spectrometer, JP500 (JPscientific, Jiangsu, China) for As and XR700 (JPscientific, Jiangsu, China) for Cd. In addition, the prepared soil samples were used to quantitatively determine the As and Cd fractions using BCR sequential extraction. Four fractions (the soluble fraction, Fe/Mn (oxyhydro)oxides fraction, organically bound and sulfide fraction, and residual fraction) were extracted sequentially based on the procedure outlined in a previous study [28]. The extraction solution was used to determine the concentrations of Cd and As using the ICP-MS and the XRF-JP500, respectively. The detection limits of XRF-JP500 for soil and solution As were 0.04 mg/kg and 0.01 mg/L, respectively, and the detection limits of XRF-XR700 for soil and solution Cd were 0.015 mg/kg and 0.01 mg/L, respectively. The recovery rate of the elements ranged between 90 and 110%.

2.2.3. DOM Characteristic

The concentration of dissolved organic carbon (DOC) of the porewater filtered through a 0.45 μm filter membrane, which represented the amount of DOM, was quantified by an automated TOC analyzer (TOC-L, Shimadzu Scientific Instruments, Kyoto, Japan) with a detection limit of 4.00 μg/L [29]. The ultraviolet–visible (UV-vis) absorption and the three-dimensional excitation–emission matrix spectroscopy (3D-EEMs) were determined using an Aqualog® fluorescence spectrophotometer (Jobin Yvon, Horiba, Kyoto, Japan) using the detailed method as described by Jang et al. [30,31]. UV-vis absorption spectroscopy was performed as follows: with Milli-Q® water as a blank, the absorbance of DOM in the porewater was measured in the range of 230–800 nm with a 1 nm interval using a

1 cm quartz colorimetric dish. The 3D-EEMs method was performed using the following instrument settings: a range of the excitation wavelength (Ex) of 200–450 nm with a 5 nm interval and a range of emission wavelength (Em) of 220–620 nm. Using Milli-Q®Water (18.2 MΩ·cm) as a blank, Raman scattering peaks were automatically corrected by Aqualog® software (2013) [30]. Four indices, including the absorption coefficient at 355 nm (α(355)), $SUVA_{254}$, $SUVA_{260}$, and the humification index (HIX), were selected to characterize the DOM structure. The definition, calculation process, and interpretation of the DOM characteristic parameters are shown in Table S1. The fluorescence regional integration (FRI) theory method divides the 3D-EEMs diagram into five subregions. The subregion results and the corresponding components are shown in Table S2.

2.3. Data Analysis

The pe + pH value is a crucial parameter to evaluate the redox state of the paddy soil environment [32]. The pe + pH value was calculated using the following equation: pe + pH = pH + Eh (mV)/59.2 [9]. The ratio of dissolved elements in porewater to the total elements gives the percentage of dissolved elements in porewater. The trade-off value of As and Cd in porewater is defined as the sum of $[Cd_p]/[Cd_{p\ max}]$ and $[As_p]/[As_{p\ max}]$. Cd_p and As_p represent the total Cd and As concentrations in porewater, and $Cd_{p\ max}$ and $As_{p\ max}$ express the maximum of the total Cd and As concentrations in porewater, respectively [3,16]. All results are presented as the mean ± standard error (Mean ± SE, n = 3). The significance levels at 0.05 were determined using Tukey's test to compare the differences between treatments. Origin Pro2023 software was used for graphing and statistical analysis (such as a one-way ANOVA and nonlinear/linear regression). Microsoft Excel 2016 software was utilized to manage the experimental data in this study.

3. Results and Discussion

3.1. Dynamic Changes in the Dissolution of As and Cd During Flooding

As illustrated in Figure 1, the flooding process had remarkable impacts on soil Eh, pH, Fe, Mn, DOC, Cd, and As concentrations in the porewater of paddy fields. During the submerged period (28 days), the soil Eh decreased from 243.7 mV to −114.5 mV (Figure 1A), the soil pH increased gradually from 5.93 to 6.81 (Figure 1B), and the pe + pH decreased from 10.05 to 4.74, similar to the variation in soil Eh (Figure 1C). Throughout the incubation process, the pe + pH decreased by five units, suggesting that the soil Eh value contributed more to the variation in the pe + pH than the soil pH. As seen in Figure 1D, once flooding was applied, the total Cd concentration in the porewater showed a markedly decreasing trend from 3.89 μg/L to 0.22 μg/L. However, the concentrations of As, Fe, and Mn in the porewater showed gradual changes with the extension of the flooding time (Figure 1E–G), varying from the detection limit (0.01 mg/L) to 0.23 mg/L, from the detection limit (0.01 mg/L) to 106.81 mg/L, and from 0.60 mg/L to 20.30 mg/L, respectively. To understand the partition characteristics of Fe, Mn, DOC, As, and Cd in porewater, concentrations of dissolved Fe, Mn, As, Cd, and DOC in porewater under a flooded status were analyzed, as shown in Figure 1H and Figure S3. Changes in the dissolved Fe, Mn, As, and DOC in the porewater exhibited similar tendencies; that is, their concentrations in the porewater gradually increased with the decrease in the pe + pH. However, with the continuous flooding process, the reducibility of the soil–porewater system became more robust, and the dissolved Cd content in the porewater decreased abruptly, starting on the sixth day of the incubation period (Figure S3A). Percentages of dissolved As and Cd compared to the total amounts of As and Cd in the porewater were 61.82% and 70.26%, respectively, as seen in Figure S3E. This result indicated that the As and Cd in the porewater mainly existed as dissolved fractions (<0.45 μm). The elevated total As concentration in the porewater was observed when the soil Eh fell below 62 mV (Figure 1A,E), and the concentration rapidly increased when the soil Eh decreased to −104 mV. This was accompanied by parallel increases in the Fe/Mn (Figure 1F,G and Figure S3C,D) and DOC concentrations in the porewater (Figure 1H). The total Cd concentration in the porewater dramatically decreased when the soil Eh was below 62 mV and slightly decreased when

the soil Eh fell below −118 mV. These results are consistent with earlier research that showed that the dissolution of As from Fe/Mn (hydr)oxides in paddy soils occurred below −100 mV [33] and the dissolution of Cd from the oxidation of sulfides happened above −100 mV [27]. By examining the relationships between the dissolved As and Cd concentrations and the Eh and pH levels, a threshold Eh of −100 to 0 mV for dissolved As and a threshold Eh of −100 mV for dissolved Cd in the porewater were identified [16]. However, our research results showed that the porewater Cd abruptly decreased at 60 mV, and the redox potential did not reach the reduction condition of sulfide (−100 mV) [22,27]. These results suggest that the rapid decrease in the Cd content of porewater at a soil Eh of 60 mV is not caused primarily by the reduction of sulfates to form sulfides and is most likely controlled by the reduction of iron and manganese oxides. Continuous flooding can result in the sequential reduction of soil Fe and S. The Fe reduction process (pe + pH = 7.66–2.80) resulted in a rapid increase in the As concentration and a sharp decrease in the Cd concentration in the soil solution. Afterward, the S reduction process (pe + pH = 2.80–2.27) caused a sharp decline in the As concentration and a further decrease in the Cd concentration in the soil solution [22]. These results show that the reduction of Fe/Mn (oxyhydro)oxides and the dissolution of DOM are consistent with the dissolution of As and occur in opposition to the dissolution of Cd in paddy soils during the flooding period.

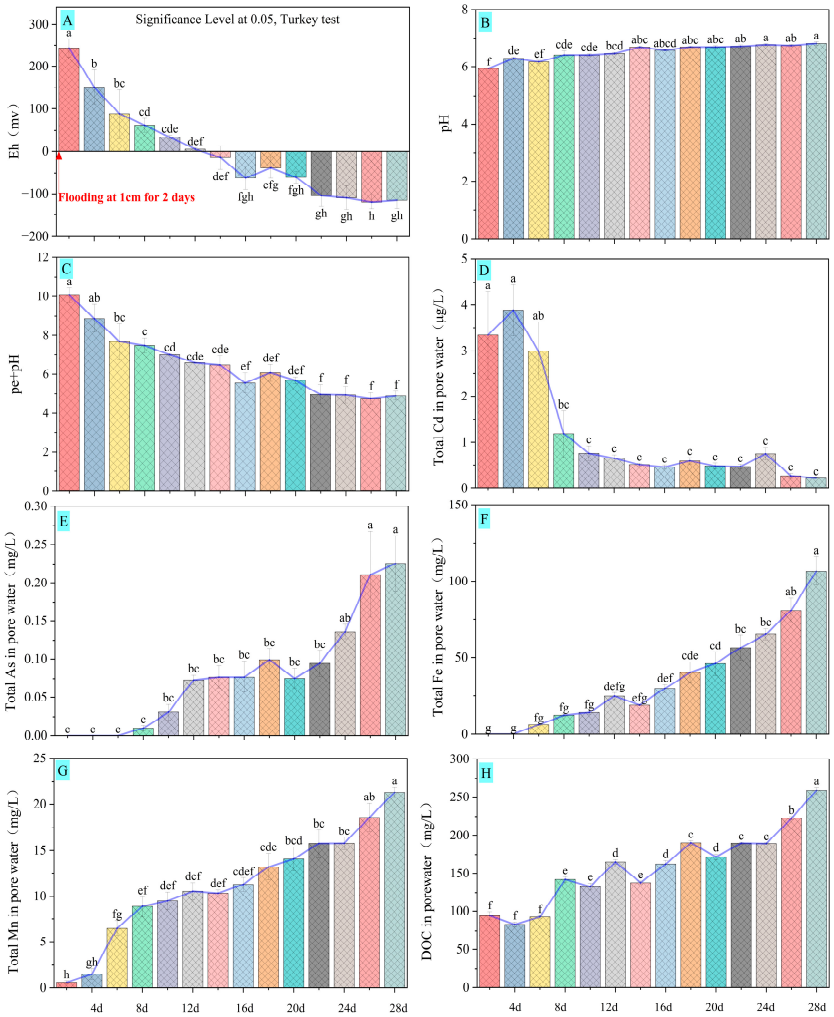

Figure 1. As and Cd dissolution characteristics under the continuous flooding incubation. (**A**–**C**) shows the dynamic change in soil pH, Eh, and pe + pH in paddy soils during flooding. (**D**–**H**) shows the dynamic changes in soil porewater Cd, As, Fe, Mn, and DOC in paddy soils during flooding. Small letters above the columns represent significant differences at the 0.05 level.

3.2. Response of As and Cd Dissolution to the Flooding Depth

This study further performed a flooding depth experiment to understand the dissolution characteristics of As and Cd, as illustrated in Figures 2 and 3. There were no significant differences in the pe + pH of paddy soils among treatments with flooding depths of 0–8 cm ($p > 0.05$). The pe + pH range of two to three under flooding depths of 0–8 cm suggests that the redox state of continuously submerged paddy soils is relatively stable. Meanwhile, there was a significant difference in the pe + pH of paddy soils between the flooding depth of 0–8 cm treatments and the dry2/dry3 treatments ($p < 0.05$) (Figure 2A). These results indicate that the effect of the flooding depth on the redox of paddy soils is not apparent when the soil surface continues to be submerged by overlying water. Meanwhile, these results also clarified that the pe + pH of paddy soils increased dramatically once the water level fell below the soil surface. As seen in Figure 2B, the total As concentration in the porewater significantly increased from 0.59 mg/L to 1.64 mg/L ($p < 0.05$) when the flooding depth varied from 8 cm to 0 cm (pe + pH from 2.37 to 2.90) and significantly decreased from 1.64 mg/L to 0.47 mg/L ($p < 0.05$) when the water management varied from the wetting to draining state (pe + pH from 3.00 to 6.88). The linear slopes of the total As in the porewater versus the soil pe + pH were 1.077 ($R^2 = 0.438$, ** $p = 0.002$) for the low pe + pH and −0.222 ($R^2 = 0.896$, * $p = 0.015$) for the high pe + pH (Figure S4B), indicating that a continuous low pe + pH (<3) promoted the release of soil As and a high pe + pH (>3) can inhibit the dissolution of soil As. Overall, the total Fe and Mn variation was similar to the total As in the porewater under various flooding depths (Figure 2D,E). In detail, there were no significant differences in the total Fe and Mn concentrations among the various flooding depth treatments (from 8 cm to 1 cm). Long-term flooding at different depths (from 8 cm to 1 cm) could intensify the dissolution of As but had little effect on the dissolution of Fe and Mn in paddy soils. Notably, the dramatic changes in the dissolution and mobility of As, Fe, and Mn from paddy soils to porewater occurred when the soil changed from flooded to drained. Generally, the total Cd in the porewater gradually increased from 0.29 μg/L to 0.90 μg/L ($p < 0.05$) during the entire period (Figure 2C) and was consistent with the changing tendency in the pe + pH (Figure 2A). Further, the linear slopes of the two sections for total Cd versus pe + pH were 0.205 ($R^2 = 0.732$, *** $p < 0.001$) for a low pe + pH of <3.5 and 0.061 ($R^2 = 0.799$, $p = 0.296$) for a high pe + pH of >3.5, respectively (Figure S4A). These results suggest that the gradual decrease in the overlay water depth from 8 cm to 1 cm (the continuous flooding condition) was conducive to Cd migration and dissolution in paddy soils despite no significant difference in the pe + pH. Similar to the As dissolution, the Cd dissolution and mobility increase were induced by considerable variation in redox when the soil changed from flooding to drainage conditions.

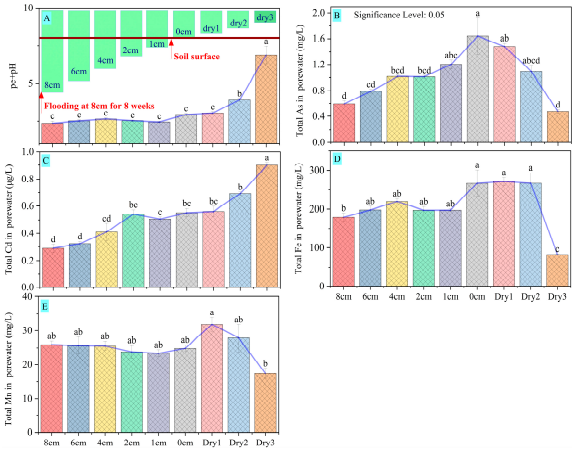

Figure 2. Dissolution characteristics of As and Cd under various flooding depths. (**A**) represents the effect of flooding depths on the pe + pH of paddy soils. (**B**–**E**) shows the impact of the flooding depths on the total As, Cd, Fe, and Mn in the porewater of paddy soils. Small letters above the columns represent significant differences at the 0.05 level.

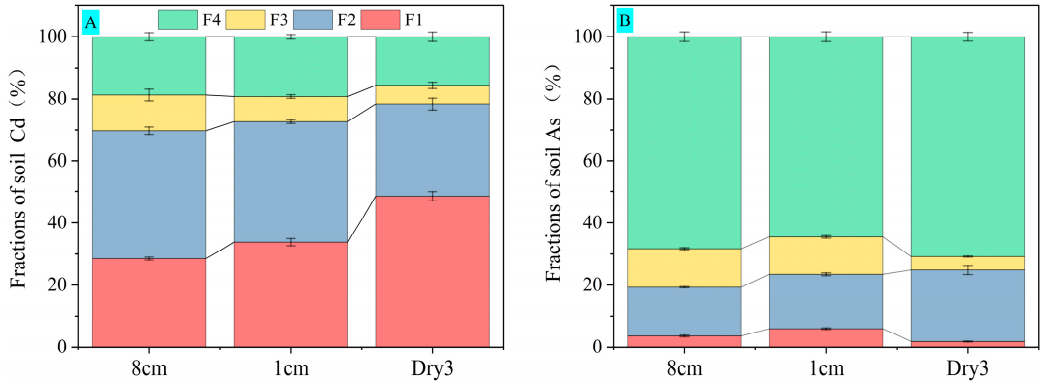

Figure 3. Effects of the flooding depths on Cd (**A**) and As (**B**) fractions in paddy soils. F1 represents the weak acid soluble fraction, F2 represents the reducible fraction (Fe/Mn (oxyhydro)oxide fraction), F3 represents the oxidizable fraction (organically bound and sulfide fraction), and F4 represents the residual fraction.

Water management is usually applied to regulate the activities of toxic elements in the paddy field based on the chemical speciation and associated transformation of these elements under different redox conditions. This study further evaluated the As and Cd fractions (chemical speciations) in paddy soils under three water management conditions (i.e., 8 cm, 1 cm, and dry3), as shown in Figure 3. With the decrease in the depths of overlay water and porewater, the weak acid-soluble Cd (the soluble fraction of Cd) in paddy soils increased from 28% to 48%, and the Fe/Mn (oxyhydro)oxide fractions and organically bound and sulfide fractions decreased from 41% to 30% and from 11% to 6%, respectively. These results illustrate that when the state of the soil changed from flooded to drained, the Fe/Mn oxyhydroxide fraction and organically bound and sulfide fractions of Cd (F2 and F3) transformed into soluble Cd (F1). Changes in the dissolution characteristics of Cd largely depend on the transformation of Cd chemical speciation between the Fe/Mn (oxyhydro)oxide fraction and the soluble fraction during the soil flooding and drainage process. However, Cd combined with sulfide and organic matter contributed less to the immobilization of Cd in paddy soils whether the soil was flooded or drained according to the proportion of F3, and this result was consistent with previous research [28,34]. Recent research has also found that the specifically adsorbed fraction of Cd and the Cd bound to Fe/Mn (oxyhydro)oxides in flooded paddy soils exhibit increasing tendencies with a decrease in the pe + pH from 7.66 to 2.8; an S reduction induced the increase in the proportion of Cd immobilized by organic matter/sulfide with a low pe + pH of 2.27–2.80 but accounts for a small percentage [22]. Other research has also indicated that a pe + pH range of 4.45–6.50 is an optimal redox condition for maximum Cd sulfide precipitation in paddy soils [20]. Under flooding condition, the lower pe + pH usually contributes to the Fe(III) reduction and Fe^{2+} increase in the soil–porewater system, which promotes Cd sequestration in amorphous Fe-oxides (amFeox-Cd), resulting in the decrease in the $CaCl_2$-extractable Cd content of paddy soils [9]. The immobilization mechanism of soil Cd could be explained by the adsorption of original Fe/Mn (oxyhydro)oxides or the coprecipitation with the newly formed Fe (oxyhydro)oxides from the anaerobic oxidation of Fe(II) in paddy soils, instead of the formation of Cd sulfides [35], and this mechanism was proved through sequential extraction and X-ray absorption spectroscopy (XAS) analyses [10].

As shown in Figure 3B, the predominant fraction of As in the tested soils was the F4 fraction (residual fraction), accounting for more than 60%. Moreover, the organically bound and sulfide fractions in paddy soils decreased from 12% to 4%; the Fe/Mn (oxyhydro)oxides fraction increased from 16% to 23%; and the order of the percentages of weak acid-soluble As (the soluble fraction of As) was 1 cm (6%) > 8 cm (3%) > dry3 (2%). The simultaneous increase in the total As and Fe concentrations in the porewater during the flooding period (Figure 2) and the suppression in the formation of the Fe/Mn (oxyhy-

dro)oxides containing As with the flooding depths of 8 cm and 1 cm (Figure 3) indicate that the continuous flooding of paddy soils usually involves the reduction and dissolution of Fe (oxyhydro)oxides, which mediate the release of As. Previous research illustrated that three fractions of soil As—(1) As precipitated with carbonates and Mn oxides, (2) As incorporated into ammonium iron (oxyhydro)oxides, and (3) As coprecipitated with pyrite and amorphous As_2S_3—exhibited apparent rising trends under the anaerobic environment, but the As incorporated into crystalline Fe (oxyhydro)oxides showed a significant decreasing trend [22]. The flooding treatment elevated the specifically sorbed or strongly adsorbed As and reduced the amorphous Fe (oxyhydro)oxides-bound As, compared to the non-flooded conditions with 60% saturated volumetric water [36].

From the above results and discussion, it can be seen that the reduction dissolution–oxidation deposition process of Fe/Mn (oxyhydro)oxides in paddy soils is a double-edged sword in regulating the availability of As and Cd in paddy soils. Under flooded conditions, the formation of the high content of amorphous Fe-oxides immobilizes the available Cd in paddy soils; the reduction dissolution of Fe (oxyhydro)oxides, inducing the low content of crystalline Fe-oxides, enhances the As availability in paddy soils [9,22]. Meanwhile, the availability of As and Cd in paddy soils were primarily controlled by soil Fe and Mn oxides, as shown in previous research [10,22,28]. In addition, the SOC and sulfur also affected the availability of As and Cd in paddy soils (Figure 3) via coprecipitation with pyrite and amorphous As_2S_3 [22] and CdS and organic-matter-bound Cd [37]. Overall, the sustained flooding resulted in a low pe + pH and strengthened the Cd immobilization in paddy soils by forming stable compounds, such as CdS or amFeox-Cd [11,32,38].

3.3. DOM Characteristics in Porewater During the Duration of the Flooding

During the flooding period (0–28 days), the DOC in porewater gradually increased from 94.11 ± 8.85 mg/L to 259.03 ± 7.92 mg/L, as illustrated in Figure 1H. The DOM showed an increasing trend with a decrease in soil redox potential. To better examine the characteristics of the DOM, the soil-derived DOM characteristics (the absorption coefficient, $SUVA_{254}$, $SUVA_{260}$, HIX, and 3D-EEMs) were calculated and are shown in Figure 4. With the extension of the flooding period, the absorption coefficient and absorbance of the porewater solution increased. The parameter $\alpha(355)$ of the porewater solution on the 4th, 10th, 20th, and 28th days was 4.14, 14.69, 19.24, and 40.35 m^{-1} (Figure 4A), respectively. This result shows an increasing concentration of chromophoric dissolved organic matter (CDOM) in porewater, representing a classification of an absorbent component rich in humic-like and protein-like substances [30]. The parameters $SUVA_{254}$ and $SUVA_{260}$ in Figure 4B represent the changing characteristics of the aromaticity and hydrophobicity of DOM in porewater during the flooding period. Values of both indicators generally exhibit a positive correlation [39]. As seen in Figure 4B, $SUVA_{254}$ and $SUVA_{260}$ showed a consistent increasing trend in this study. The tendency indicated that the aromaticity and hydrophobicity of DOM in porewater increased gradually with the prolongation of flooding. The degree of humification of DOM showed the following order: 28th day > 20th day > 10th day > 4th day, consistent with the change in the DOC concentration and UV spectrum analysis ($\alpha(355)$, $SUVA_{254}$, and $SUVA_{260}$), implying that the degree of humification of DOM is promoted by flooding status. The increased HIX of DOM in porewater with the extension of the flooding period indicated that the molecular composition of DOM tended to be complicated, possibly due to the activation and promotion of the humification of organic matter by soil microorganisms under a continuously flooded environment [40].

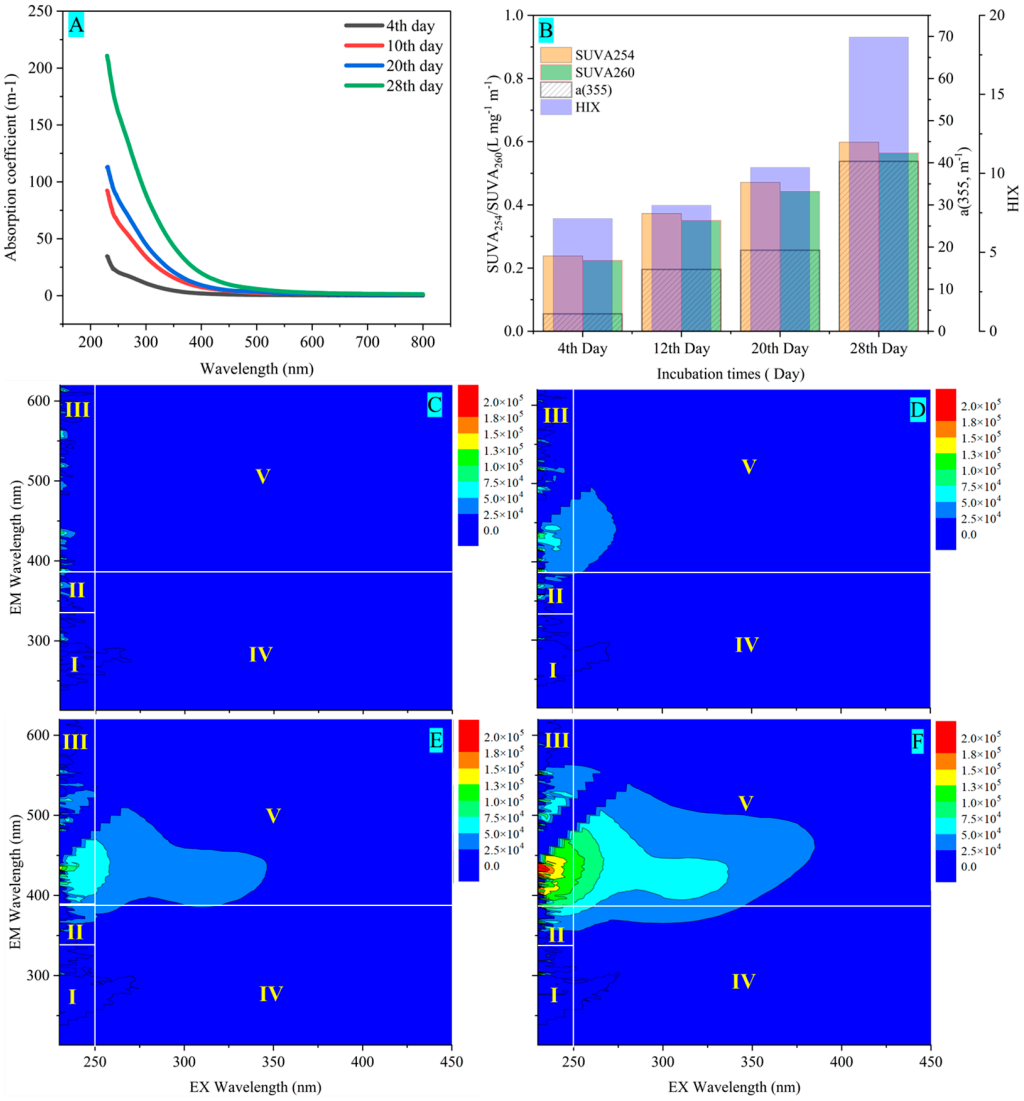

Figure 4. UV-vis and 3D-EEMs characteristics of DOM in paddy soils during flooding incubation. (**A**) represents the absorption coefficient of DOM for the UV-vis spectrum. (**B**) represents the UV spectral characteristic parameters (a(355), $SUVA_{254}$, and $SUVA_{260}$) and the fluorescence spectral characteristic parameters (HIX). (**C**–**F**) represents the 3D-EEMs diagrams of DOM on the 4th, 12th, 20th, and 28th days of the flooding period, respectively. I–V of five subregions represent tyrosine, tryptophan, fulvic acids, soluble microbial by-products, and humic acids, respectively.

The fluorescence contour plots of the DOM were divided into five sections according to the FRI method. With the increased flooding time, the fluorescence intensity of DOM in porewater increased gradually (Figure 4C–F). The major peaks in 3D-EEMs were identified, and there were four prominent peaks: peak A (λ_{ex} = 200–215 nm; λ_{em} = 300–325 nm), peak B (λ_{ex} = 200–215 nm; λ_{em} = 360–400 nm), peak C (λ_{ex} = 250–300 nm; λ_{em} = 325–425 nm), and peak D (λ_{ex} = 300–340 nm; λ_{em} = 370–430 nm). This study observed two prominent peaks (peaks B and D) (Figure 4F). The fluorescence intensity of peak B (denoted as Region III) increased, showing an increase in fulvic acid substances from the 4th to the 28th day. The intensity of peak D (denoted as Region V) appeared with an increasing submerged culture time, indicating that long-term flooding promoted the formation of humic acid matter [39]. These results show that the reducing environment caused by flooding promoted the humification process of the SOC in paddy soils. The fluorescence intensities of the I, II, and IV regions, which represent the tyrosine, tryptophan, and soluble microbial by-products, were fragile during the submerged culture. This result suggests that the metabolic

process of microorganisms and the decomposition process of organic matter dependent on the microorganisms were not apparent during the flooding cycle. The humification process of the SOC may provide additional electrons for the soil environment to regulate the reductive process of Fe/Mn oxides and sulfide and further control the As and Cd availability in paddy soils [13,14,22]. Soils with a low pe + pH could facilitate the dissolution of electron-acceptable substances (DOM) [13,36]. Additionally, humic substances, acting as electron shuttles, promote Fe and As reductions [13,41], and the extent of As reduction by these substances is given in the following order: fulvic acid > humic acid > humin [13].

3.4. Optimal pe + pH for Simultaneously Decreasing Dissolved As and Cd

As mentioned above, the reduction and dissolution of Fe/Mn (oxyhydro)oxides, the humification of the SOC, the reduction of arsenate, and the availability of As and Cd in paddy soils are highly related to the water management process. Variations in Fe, Mn, DOC, As, and Cd concentrations in porewater are the function of soil redox parameters that present synchronously. Therefore, we conducted correlation and cluster analyses, as shown in Figure 5. On the one hand, variations in the soil Eh (R = 0.78, ** p < 0.01) and pe + pH (R = 0.77, ** p < 0.01) significantly and positively influenced the Cd concentration in porewater. This result indicates that soil with a reducing condition could effectively mitigate the Cd dissolution in paddy soils. On the other hand, varying the soil pe + pH significantly and negatively affected the concentrations of As (R= −0.72, ** p < 0.01), Fe (R = −0.79, ** p < 0.01), Mn (R = −0.90, ** p< 0.01), and DOC (R = −0.84, ** p < 0.01) in porewater (Figure 5A). These results indicate that the flooding process enhanced the soil reduction capacity and led to the consistent dissolution characteristics of As, Fe, Mn, and DOC. A heat map with normalized concentrations also confirmed the above results (Figure 5B). In detail, the dissolution characteristics of As, Fe, Mn, and DOC in the porewater form one group, while Cd is another independent group; their dissolution and mobility processes are opposite under the draining environment.

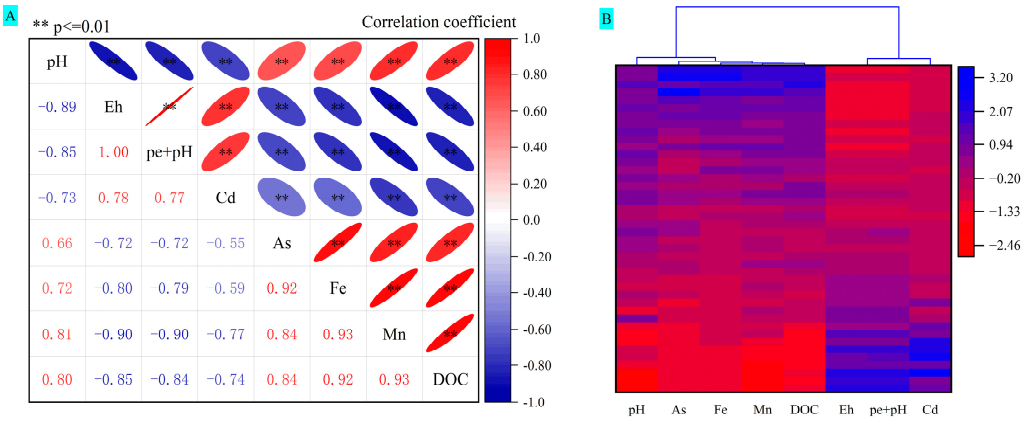

Figure 5. Pearson correlation analysis (**A**) and cluster analysis (**B**) among the soil pH, Eh, pe + pH, Cd, As, Fe, Mn, and DOC. Significant correlation is confirmed using the p-value at 0.01 levels (** p < 0.01). The approach of cluster analysis is based on the correlation coefficient.

The pe + pH (pH + Eh(mV)/59.2) is a parameter characterizing the redox reaction in paddy soils. It can be used to evaluate the dynamic changes in Fe/Mn oxides in paddy soils and their adsorption and fixation capacities for heavy metals. The pe + pH represents the redox state of paddy soils: the greater the value, the less reducibility of the soil environment. According to the classification of reduction states for paddy soil, pe + pH < 5 is intense reduction, 5 < pe + pH < 7.25 is moderate reduction, and 11.34 < pe + pH < 14 is weak reduction [42]. Figure 6 shows the relationships of the total Cd, As, Fe, Mn, and DOC concentrations in porewater and the trade-off value of the normalized total As and Cd concentrations versus soil pe + pH. The total Cd in the porewater dramatically increased with the increase in the pe + pH and maintained a low concentration when the pe + pH was

below 6.5 (Figure 6A). In contrast, the total As concentration in the porewater decreased with an increasing pe + pH and was negligible at a pe + pH of >7 while it increased sharply when the pe + pH was below 5 (Figure 6B). The Fe, Mn, and DOC in the porewater showed similar relationships with the pe + pH (Figure 6C–E), confirmed by the positive correlations (Figure 5A) and the cluster analysis results (Figure 5B).

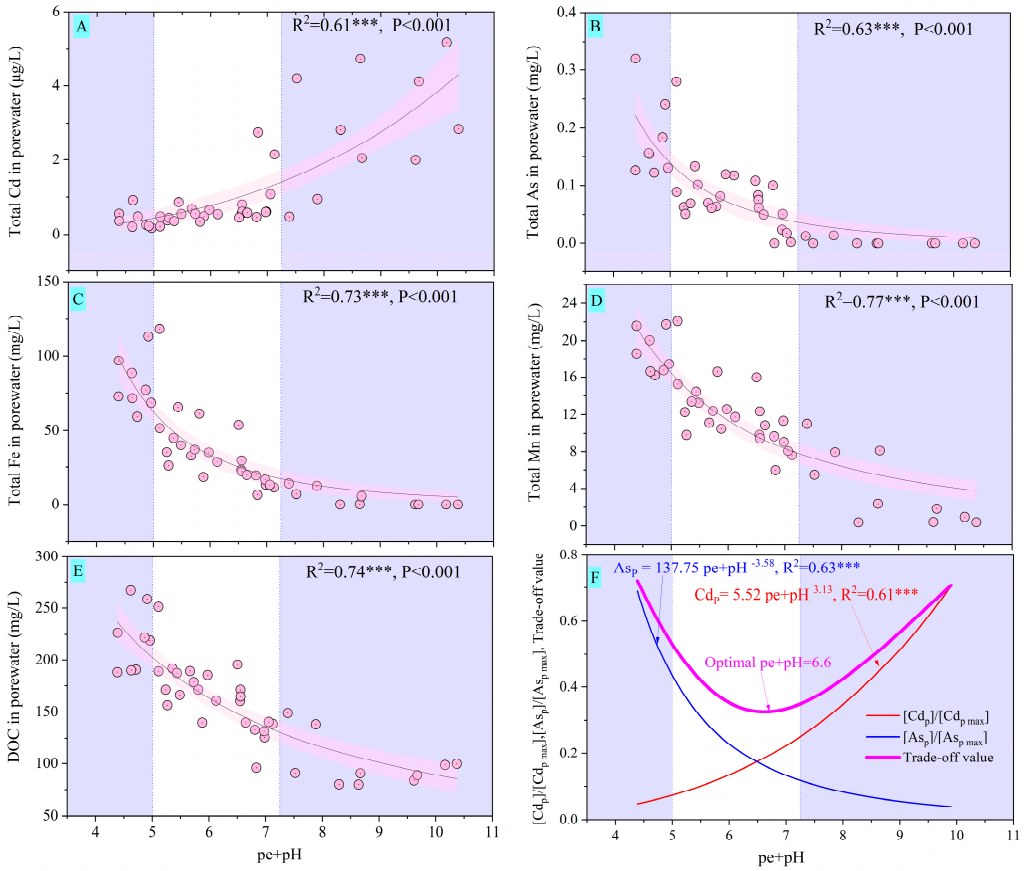

Figure 6. Quantitative relationships between total/dissolved elements/substances in porewater and pe + pH. (**A**–**E**) show the nonlinear fitting results of the total Cd, As, Fe, Mn, and DOC concentrations versus pe + pH in the porewater of paddy soils. (**F**) shows the trade-off value of the normalized total Cd and As concentrations in porewater of paddy soils versus pe + pH. The trade-off value is defined as the sum of $[Cd_p]/[Cd_{p\ max}]$ and $[As_p]/[As_{p\ max}]$. *** indicates that pe + pH has a significant effect on the response indicator at the 0.001 level.

Because As and Cd have opposite geochemical characteristics, many porewater samples showed high As and low Cd concentrations or low As and high Cd concentrations. Meanwhile, the data showing a combination of low As and Cd concentrations in porewater with a pe + pH of 5–7.25 (weak reduction) can be seen in Figure 6A,B. These results suggest that an optimal soil Eh and pH may exist, which can facilitate a low As and Cd dissolution and further inhibit rice uptake in paddy soils co-contaminated with As and Cd. In this study, the dataset of the total concentrations of As and Cd in porewater during flooding (Experiment 1) was used to calculate the trade-off of both elements. The trade-off calculation for the total As and Cd concentrations in porewater was introduced in Section 2.3. The relationships of $[As_p]/[As_{p\ max}]$, $[Cd_p]/[Cd_{p\ max}]$, and the trade-off value versus the pe + pH are shown in Figure 6F. This study obtained the minimum trade-off at the optimal pe + pH of 6.6, which belongs to the moderate reduction status. Relevant research found optimal pe + pH values of 3.25 [22], 4.6 [3], 5.1 [18], and 5.0 [16], which are shown in Table S3. The redox status mainly concentrates on the distribution of the intense reduction status (pe + pH < 5) or close to the moderate reduction status (5 < pe + pH < 7.25). The results of this study were slightly different from those of other studies. The possible

reasons for this are as follows: (1) this study used the comprehensive index of redox status (pe + pH) as the independent variable to conduct a nonlinear regression analysis of the trade-off value, while other studies used soil pH or Eh as the independent variable to conduct nonlinear regression analyses individually, and (2) there were differences in the physicochemical characteristics (the pH, SOC, As, and Cd concentrations and availability) of paddy soils and different experimental conditions (such as the extraction method of As and Cd), as shown in Table S3. Generally, the trade-off value could be a valuable indicator for identifying the optimum soil pe + pH. However, we should realize that $[As_p]/[As_{p\ max}]$ and $[Cd_p]/[Cd_{p\ max}]$ versus the pe + pH are specific to the characteristics of paddy soils and that the optimum Eh, pH, and pe + pH may vary with the experimental conditions [16,22] and soil types [3]. The critical question is how to use the optimal pe + pH value to construct water management measures to guide agricultural practice. For example, compared to regular cultivation, soil ridge cultivation may have great potential to regulate the optimal pe + pH to reduce As and Cd availability in paddy soils, further reducing the accumulation of As and Cd in rice tissues [24].

4. Conclusions

This study discussed the effect of flooding and drainage on As and Cd availability in paddy soils via a microcosm experiment system. The reduction of Fe/Mn (oxyhydro)oxides is consistent with As dissolution and occurs in opposition to Cd dissolution in paddy soils during flooding and subsequent drainage. The reduction dissolution–oxidation deposition process of Fe/Mn (oxyhydro)oxides is a double-edged sword in regulating As and Cd availability in paddy soils. Whether the tested soils are flooding or draining, Fe/Mn (oxyhydro)oxides always play a vital role in regulating the Cd availability relative to sulfide. In addition, the Fe/Mn (oxyhydro)oxide fraction and the organically bound and sulfide fractions together determine the As availability in paddy soils. With the 3D-EEMs of DOM, flooding promotes the humification of the SOC of paddy soils, which further facilitates the reduction of Fe/Mn (oxyhydro)oxides and increases the availability of soil As. In addition, the optimal pe + pH response to the minimum trade-off value of the total As and Cd in porewater was found to be 6.6, which indicates a moderate reduction status. Further work is needed to determine how the optimal pe + pH value can be used to construct water management measures with a moderate reduction status for agricultural practice.

Supplementary Materials: The following supporting information can be downloaded at https://www.mdpi.com/article/10.3390/agriculture14111933/s1: Figure S1: Experiment design of different flooded times (Experiment 1); Figure S2: Experiment design of different flooded depths (Experiment 2); Figure S3: Dissolution characteristics of dissolved elements/substances in porewater of paddy soils during the flooding period; Figure S4: Quantitative relationships between total Cd/As in porewater and soil redox capacity (pe + pH) under different flooding depths; Table S1: The definition and significance of the DOM characteristic parameters; Table S2: Subregions of 3D-EEMs according to the FRI theory and the corresponding components; Table S3: The minimum trade-off of As and Cd in soils corresponds to the optimal pH, Eh, and pe + pH.

Author Contributions: X.T., conceptualization, data curation, visualization, software, writing—original draft preparation, funding acquisition, visualization, and supervision; J.L., investigation, data curation, software, and visualization; G.C., conceptualization, methodology, formal analysis, and supervision; D.L., writing—review and editing; Y.G., writing—review and editing; H.L., writing—review and editing; Q.X., formal analysis, data curation, and writing—review and editing; G.L., conceptualization and writing—review and editing. All authors have read and agreed to the published version of the manuscript.

Funding: This research was funded by the Natural Science Foundation of Chongqing (CSTB2022NSCQ-MSX0563) and the Science and Technology Research Program of Chongqing Municipal Education Commission (KJZD-K202203401 and KJZD-K202303402).

Institutional Review Board Statement: Not applicable.

Data Availability Statement: The data presented in this study are available upon request from the corresponding author.

Acknowledgments: The authors gratefully thank Yongmin Wang and Tao Jiang for their assistance with the experimental instruments.

Conflicts of Interest: The authors declare that they have no known competing financial interests or personal relationships that could have appeared to influence the work reported in this paper.

References

1. Dai, J.; Tang, Z.; Gao, A.X.; Planer-Friedrich, B.; Kopittke, P.M.; Zhao, F.J.; Wang, P. Widespread occurrence of the highly toxic dimethylated monothioarsenate (DMMTA) in rice clobally. *Environ. Sci. Technol.* **2022**, *56*, 3575–3586. [CrossRef] [PubMed]
2. Zhao, F.J.; McGrath, S.P.; Meharg, A.A. Arsenic as a food chain contaminant: Mechanisms of plant uptake and metabolism and mitigation strategies. *Annu. Rev. Plant Biol.* **2010**, *61*, 535–559. [CrossRef] [PubMed]
3. Yao, B.M.; Wang, S.Q.; Xie, S.T.; Li, G.; Sun, G.X. Optimal soil Eh, pH for simultaneous decrease of bioavailable Cd, As in co-contaminated paddy soil under water management strategies. *Sci. Total Environ.* **2022**, *806*, 151342. [CrossRef] [PubMed]
4. Zhao, F.J.; Wang, P. Arsenic and cadmium accumulation in rice and mitigation strategies. *Plant Soil* **2020**, *446*, 1–21. [CrossRef]
5. Ali, W.; Mao, K.; Zhang, H.; Junaid, M.; Xu, N.; Rasool, A.; Feng, X.B.; Yang, Z.G. Comprehensive review of the basic chemical behaviours, sources, processes, and endpoints of trace element contamination in paddy soil-rice systems in rice-growing countries. *J. Hazard. Mater.* **2020**, *397*, 122720. [CrossRef]
6. Carrijo, D.R.; LaHue, G.T.; Parikh, S.J.; Chaney, R.L.; Linquist, B.A. Mitigating the accumulation of arsenic and cadmium in rice grain: A quantitative review of the role of water management. *Sci. Total Environ.* **2022**, *839*, 156245. [CrossRef]
7. Yang, Q.Q.; Li, Z.Y.; Lu, X.N.; Duan, Q.N.; Huang, L.; Bi, J. A review of soil heavy metal pollution from industrial and agricultural regions in China: Pollution and risk assessment. *Sci. Total Environ.* **2018**, *642*, 690–700. [CrossRef]
8. Chen, H.P.; Yang, X.P.; Wang, P.; Wang, Z.X.; Li, M.; Zhao, F.J. Dietary cadmium intake from rice and vegetables and potential health risk: A case study in Xiangtan, southern China. *Sci. Total Environ.* **2018**, *639*, 271–277. [CrossRef]
9. Li, S.S.; Lei, X.Q.; Qin, L.Y.; Sun, X.Y.; Wang, L.F.; Zhao, S.W.; Wang, M.; Chen, S.B. Fe(III) reduction due to low pe + pH contributes to reducing Cd transfer within a soil-rice system. *J. Hazard. Mater.* **2021**, *415*, 125668. [CrossRef]
10. Wang, J.; Wang, P.M.; Gu, Y.; Kopittke, P.M.; Zhao, F.J.; Wang, P. Iron-manganese (oxyhydro)oxides, rather than oxidation of sulfides, determine mobilization of cd during soil drainage in paddy soil systems. *Environ. Sci. Technol.* **2019**, *53*, 2500–2508. [CrossRef]
11. Zhang, F.; Peng, R.; Wang, L.F.; Jiang, H.D. Iron and sulfur reduction caused by different growth seasons inhibits cadmium transfer in the soil-rice system. *Ecotoxicol. Environ. Saf.* **2022**, *236*, 113479.
12. Miao, F.; Zhang, X.; Fu, Q.L.; Hu, H.Q.; Islam, M.S.; Fang, L.C.; Zhu, J. Sulfur enhances iron plaque formation and stress resistance to reduce the transfer of Cd and As in the soil-rice system. *Sci. Total Environ.* **2024**, *927*, 171689. [CrossRef] [PubMed]
13. Qiao, J.T.; Li, X.M.; Li, F.B.; Liu, T.X.; Young, L.Y.; Huang, W.L.; Sun, K.; Tong, H.; Hu, M. Humic substances facilitate arsenic reduction and release in flooded paddy soil. *Environ. Sci. Technol.* **2019**, *53*, 5034–5042. [CrossRef] [PubMed]
14. Li, B.; Zhang, T.; Zhang, Q.; Zhu, Q.H.; Huang, D.Y.; Zhu, H.H.; Xu, C.; Su, S.M.; Zeng, X.B. Influence of straw-derived humic acid-like substance on the availability of Cd/As in paddy soil and their accumulation in rice grain. *Chemosphere* **2022**, *300*, 134368. [CrossRef] [PubMed]
15. Linam, F.; Limmer, M.A.; Tappero, R.; Seyfferth, A.L. Rice husk and charred husk amendments increase porewater and plant Si but water management determines grain As and Cd concentration. *Plant Soil* **2022**, *477*, 135–152. [CrossRef]
16. Honma, T.; Ohba, H.; Kaneko-Kadokura, A.; Makino, T.; Nakamura, K.; Katou, H. Optimal soil Eh, pH, and water management for simultaneously minimizing arsenic and cadmium concentrations in rice grains. *Environ. Sci. Technol.* **2016**, *50*, 4178–4185. [CrossRef]
17. Chi, Y.H.; Tam, N.F.Y.; Li, W.C.; Ye, Z.H. Multiple geochemical and microbial processes regulated by redox and organic matter control the vertical heterogeneity of As and Cd in paddy soil. *Sci. Total Environ.* **2022**, *839*, 156229. [CrossRef]
18. Shen, B.B.; Wang, X.M.; Zhang, Y.; Zhang, M.; Wang, K.; Xie, P.; Ji, H.B. The optimum pH and Eh for simultaneously minimizing bioavailable cadmium and arsenic contents in soils under the organic fertilizer application. *Sci. Total Environ.* **2020**, *711*, 135229. [CrossRef]
19. Yin, N.Y.; Li, Y.P.; Cai, X.L.; Du, H.L.; Wang, P.F.; Han, Z.L.; Sun, G.X.; Cui, Y.S. The role of soil arsenic fractionation in the bioaccessibility, transformation, and fate of arsenic in the presence of human gut microbiota. *J. Hazard. Mater.* **2020**, *401*, 123366. [CrossRef]
20. Chen, S.B.; Chen, L.; Wang, D.; Wang, M. Low pe plus pH induces inhibition of cadmium sulfide precipitation by methanogenesis in paddy soil. *J. Hazard. Mater.* **2022**, *437*, 129297. [CrossRef]
21. Yan, S.W.; Yang, J.H.; Si, Y.B.; Tang, X.J.; Ma, Y.H.; Ye, W.L. Arsenic and cadmium bioavailability to rice (*Oryza sativa* L.) plant in paddy soil: Influence of sulfate application. *Chemosphere* **2022**, *307*, 135641. [CrossRef] [PubMed]
22. Yin, Y.P.; Wang, Y.R.; Ding, C.F.; Zhou, Z.G.; Tang, X.; He, L.Q.; Li, Z.Y.; Zhang, T.L.; Wang, X.X. Impact of iron and sulfur cycling on the bioavailability of cadmium and arsenic in co-contaminated paddy soil. *J. Hazard. Mater.* **2024**, *465*, 133408. [CrossRef] [PubMed]

23. Wang, J.; Yu, L.; Qin, L.Y.; Sun, X.Y.; Zhou, W.N.; Wang, M.; Chen, S.B. Low pe + pH inhibits Cd transfer from paddy soil to rice tissues driven by S addition. *Chemosphere* **2023**, *335*, 139126. [CrossRef] [PubMed]
24. Jiku, M.A.S.; Zeng, X.B.; Li, L.Y.; Li, L.J.; Zhang, Y.; Huo, L.J.; Shan, H.; Zhang, Y.; Wu, C.X.; Su, S.M. Soil ridge cultivation maintains grain As and Cd at low levels and inhibits As methylation by changing arsM-harboring bacterial communities in paddy soils. *J. Hazard. Mater.* **2022**, *429*, 128325. [CrossRef]
25. *GB15618-2018*; Soil Environmental Quality Risk Control Standard for Soil Contamination of Agricultural Land. MEE: Beijing, China, 2018.
26. Tian, X.S.; Chai, G.Q.; Lu, M.; Xiao, R.; Xie, Q.; Luo, L.Z. A new insight into the role of iron plaque in arsenic and cadmium accumulation in rice (*Oryza sativa* L.) roots. *Ecotoxicol. Environ. Saf.* **2023**, *254*, 114714. [CrossRef]
27. Huang, H.; Chen, H.P.; Kretzschmar, R.; Zhao, F.J.; Wang, P. The voltaic effect as a novel mechanism controlling the remobilization of cadmium in paddy soils during drainage. *Environ. Sci. Technol.* **2021**, *55*, 1750–1758. [CrossRef]
28. Wu, J.Z.; Li, Z.T.; Huang, D.; Liu, X.M.; Tang, C.X.; Parikh, S.J.; Xu, J.M. A novel calcium-based magnetic biochar is effective in stabilization of arsenic and cadmium co-contamination in aerobic soils. *J. Hazard. Mater.* **2020**, *387*, 122010. [CrossRef]
29. Sun, T.; Xie, Q.; Li, C.X.; Huang, J.Y.; Yue, C.P.; Zhao, X.J.; Wang, D.Y. Inorganic versus organic fertilizers: How do they lead to methylmercury accumulation in rice grains. *Environ. Pollut.* **2022**, *314*, 120341. [CrossRef]
30. Jiang, T.; Chen, X.X.; Wang, D.Y.; Liang, J.; Bai, W.Y.; Zhang, C.; Wang, Q.L.; Wei, S.Q. Dynamics of dissolved organic matter (DOM) in a typical inland lake of the Three Gorges Reservoir area: Fluorescent properties and their implications for dissolved mercury species. *J. Environ. Manag.* **2018**, *206*, 418–429. [CrossRef]
31. Jiang, T.; Wang, D.Y.; Wei, S.Q.; Yan, J.L.; Liang, J.; Chen, X.S.; Liu, J.; Wang, Q.L.; Lu, S.; Gao, J.; et al. Influences of the alternation of wet-dry periods on the variability of chromophoric dissolved organic matter in the water level fluctuation zone of the Three Gorges Reservoir area, China. *Sci. Total Environ.* **2018**, *636*, 249–259. [CrossRef]
32. Li, S.S.; Chen, S.B.; Wang, M.; Lei, X.Q.; Han, Y. Iron fractions responsible for the variation of Cd bioavailability in paddy soil under variable pe + pH conditions. *Chemosphere* **2020**, *251*, 126355. [CrossRef] [PubMed]
33. Yamaguchi, N.; Nakamura, T.; Dong, D.; Takahashi, Y.; Amachi, S.; Makino, T. Arsenic release from flooded paddy soils is influenced by speciation, Eh, pH, and iron dissolution. *Chemosphere* **2011**, *83*, 925–932. [CrossRef] [PubMed]
34. Zhang, H.; Shao, J.G.; Zhang, S.H.; Zhang, X.; Chen, H.P. Effect of phosphorus-modified biochars on immobilization of Cu (ii), Cd (ii), and As (v) in paddy soil. *J. Hazard. Mater.* **2019**, *390*, 121349. [CrossRef] [PubMed]
35. Yu, H.Y.; Li, F.B.; Liu, C.S.; Huang, W.; Liu, T.X.; Yu, W.M. Iron redox cycling coupled to transformation and immobilization of heavy metals: Implications for paddy rice safety in the red soil of South China. *Adv. Agron.* **2016**, *137*, 279–317.
36. Das, S.; Chou, M.L.; Jean, J.S.; Liu, C.C.; Yang, H.J. Water management impacts on arsenic behavior and rhizosphere bacterial communities and activities in a rice agro-ecosystem. *Sci. Total Environ.* **2016**, *542*, 642–652. [CrossRef]
37. Qin, L.; Wang, L.; Zhao, S.; Sun, X.; Yu, L.; Wang, M.; Chen, S. A new insight into Cd reduction by flooding in paddy soil: The different dominant roles of Fe and S on Cd immobilization under fluctuant pe + pH conditions. *Sci. Total Environ.* **2022**, *847*, 157604. [CrossRef]
38. Wiggenhauser, M.; Aucour, A.-M.; Bureau, S.; Campillo, S.; Telouk, P.; Romani, M.; Ma, J.F.; Landrot, G.; Sarret, G. Cadmium transfer in contaminated soil-rice systems: Insights from solid-state speciation analysis and stable isotope fractionation. *Environ. Pollut.* **2021**, *269*, 115934. [CrossRef]
39. Ji, L.C.; Yu, Z.P.; Cao, Q.; Gui, X.Y.; Fan, X.J.; Wei, C.C.; Jiang, F.; Wang, J.; Meng, F.B.; Li, F.Y.; et al. Effect of hydrothermal temperature on the optical properties of hydrochar-derived dissolved organic matter and their interactions with copper (II). *Biochar* **2024**, *6*, 64. [CrossRef]
40. Wang, J.J.; Liu, Y.; Bowden, R.D.; Lajtha, K.; Simpson, A.J.; Huang, W.L.; Simpson, M.J. Long-term nitrogen addition alters the composition of soil-derived dissolved organic matter. *ACS Earth Space Chem.* **2020**, *4*, 189–201. [CrossRef]
41. Zhou, G.W.; Yang, X.R.; Li, H.; Marshall, C.W.; Zheng, B.X.; Yan, Y.; Su, J.Q.; Zhu, Y.G. Electron Shuttles Enhance Anaerobic Ammonium Oxidation Coupled to Iron(III) Reduction. *Sci. Total Environ.* **2016**, *50*, 9298–9307. [CrossRef]
42. Huang, D.D.; Ge, Y.; Zhou, Q.S. Effect of redox processes on soil Cd activity under submerged conditions. *Acta Sci. Circumstantiae* **2009**, *29*, 373–380. (In Chinese)